An Islanding Detection Method by Using Frequency Positive Feedback Based on FLL for Single-Phase Microgrid

Sun, Qinfei; Guerrero, Josep M.; Jing, Tianjun; Quintero, Juan Carlos Vasquez; Yang, Rengang

Published in:
I E E E Transactions on Smart Grid

DOI (link to publication from Publisher):
10.1109/TSG.2015.2508813

Publication date:
2017

Document Version
Accepted author manuscript, peer reviewed version

An Islanding Detection Method by Using Frequency Positive Feedback Based on FLL for Single-Phase Microgrid

Qinfei Sun, *Student Member, IEEE*, Josep M. Guerrero, *Fellow, IEEE*, Tianjun Jing, Juan C. Vasquez, *Senior Member, IEEE*, Rengang Yang

***Abstract*--An active islanding detection method based on Frequency-Locked Loop (FLL) for constant power controlled inverter in single-phase microgrid is proposed. This method generates a phase shift comparing the instantaneous frequency obtained from FLL unit with the nominal frequency to modify the reference phase angle. An initial low frequency variable triangular disturbance is added to the phase shift in order to reduce NDZ and accelerate the detection process especially in the case of power matching. With the modified phase angle, the frequency at PCC will be drifted away from the nominal frequency until exceeding the threshold because of the frequency positive feedback after islanding. Besides, FLL is introduced to this method in order to lock frequency quickly considering that the frequency is time-varying during the islanding detection process. Simulation and experiment have been done to evaluate this method.**

***Index Terms*--Islanding detection, frequency positive feedback, Frequency-Locked Loop (FLL), Single-phase microgrids, constant power control.**

I. Introduction

MICROGRID is a combination of various kinds of distributed generations (DGs), energy storage and controllable local loads [1].With microgrid, the negative impact to utility grid caused by DGs, e.g. power intermittent can be eliminated. Meanwhile, it can provide reliable and high quality power to local loads. In order to achieve efficient and safe performance of these small but intelligent systems, microgrids can flexibly operate both in island and grid-connected mode. But for each operation mode, the local management objectives and control methodologies are different. In island mode, the control objectives aim to guarantee reliable and high quality power supply, coordination control, energy management and so on. In grid-connected mode, the exchange power control and management between utility grid and microgrid will be concerned.

On the other hand, similar to grid-connected inverters used for DGs, safety hazard and damages will lead to personal and equipment if it's still connected to utility grid when islanding procedure occurs, particularly an unintentional one. But different from DGs which just stop working and disconnecting from grid within a short time interval (according to some standards such as IEEE std. 1547), microgrids should seamlessly transfer to island mode in order to provide voltage to local consumers. Hence, robust, fast and accurate islanding detection is critical for operation mode selection and microgrid security [2, 3].

With regards to islanding detection for grid-connected inverters, several methods were studied in literatures [2, 4-19]. Normally, islanding detection methods can be classified as communication based methods, passive methods and active methods.

Although communication based method doesn't have non-detection zone (NDZ) in theory, it relies on communication too much. Additionally, the total investment is high enough and the implementation is usually complex and difficult [2, 4].

The other two categories are both local methods. Passive methods detect islanding by monitoring local electrical parameters only, e.g. voltage, frequency, phase and harmonics at the point of common coupling (PCC). Usually, these parameters will be abnormal or change in some degree after island occurs, which will trip the detector. OUV/OUF, Voltage Harmonics, Phase Jump, ROCOF/ ROCOV/ROCOP etc. [5-10] are the most commonly used trip detectors. Passive method is easy to implement and effective in most situations. It doesn't affect power quality in grid-connected mode. However, it has a large NDZ especially when the generated power matches local consumption.

In order to reduce NDZ, active methods detect islanding by injecting disturbance such as frequency, voltage, power and harmonic intentionally [11]. Active frequency drift (AFD) method introduces slight zero chopper to output current which drifts the frequency increase/decrease after islanding. But for multiple converters and high Q load, this method would be ineffective [12]. Active frequency drift positive feedback (AFDPF) methods utilize a self positive feedback to increase zero fraction and accelerate frequency deviation. It solved the problem existed for multiple converters and reduced NDZ greatly [13]. Sandia frequency shift (SFS) is similar to AFDPF which also employs positive frequency feedback [15]. For frequency based methods, power quality will be decreased in grid-connected mode due to the existing of zero intervals. Slide mode frequency shift (SMS) methods solved this issue

This work was supported in part by the National Natural Science Foundation of China under Grant 51207160 and Grant 51477173 and in part by the Program for New Century Excellent Talents in University under Grant NCET-13-0565.

Qinfei Sun, Tianjun Jing, Rengang Yang are with College of information and Electrical Engineering, China Agricultural University, 10083 Beijing, P.R. China(e-mail:qinfeisun@cau.edu.cn; jingtianjun @126.com; yrg@cau.edu.cn).

J. M. Guerrero and J. C. Vasquez are with Department of Energy Technology, Aalborg University, 9220 Aalborg, Denmark (e-mail: joz@et.aau.dk; juq@et.aau.dk).

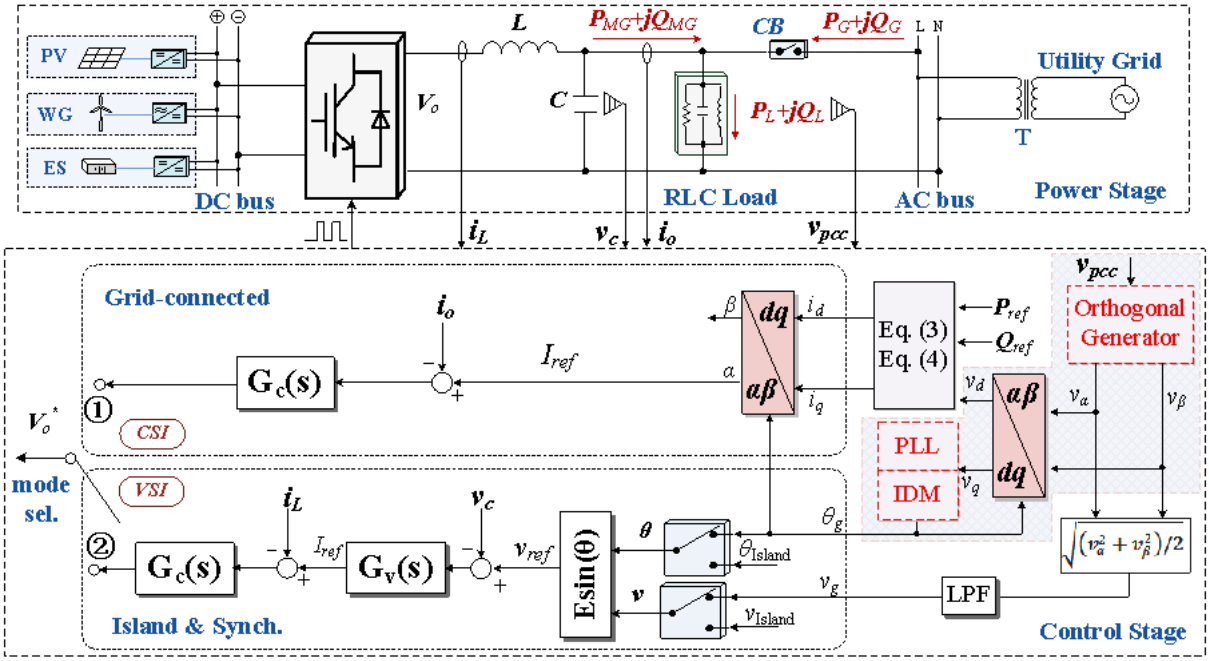

Fig. 1. Power stage and control algorithm for inverter used in single phase microgrid

by applying phase shift instead of frequency shift to remove zero intervals. However, SMS is only stimulated by an uncontrollable, externally supplied perturbation caused by noise, measurement and quantization errors in practice when the power matches well [5, 15]. Hence, the detection would cost longer time. By an initial permanent phase disturbance angle, auto phase shift (APS) method accelerates the process [16]. But it's difficult and complicated to design parameters for APS. Besides, for constant power controlled converter, the initial constant disturbance phase will be weaken or even counteracted due to power regulation [14]. Some modified SMS methods shown in [16] have the same effect as APS. For frequency and phase shift active methods, Phase-Locked Loop (PLL) is the base to generate frequency and reference phase. In [18, 19], some active methods were proposed by modifying the PLL structure. Some other active methods were introduced in [11], [20] by voltage positive feedback, power distortion and harmonic injection respectively. These active methods decrease NDZ and detection time obviously for most grid-connected inverters with constant current control. In this paper, an active islanding detection method for constant power controlled microgrid with PLL is proposed. This method applies frequency positive feedback by comparing the instantaneous frequency with nominal line frequency. Meanwhile, FLL is introduced in order to lock PCC frequency quickly considering that the frequency is time-varying during the islanding detection process. An initial low frequency triangular phase disturbance is employed. Contrast with those active methods mentioned above, it performances well both in detection time and power quality for constant power control algorithm in microgrid.

This paper is organized as follows: the basic control structure is introduced and the PCC voltage response after islanding is analyzed in Section II. In Section III, the islanding detection method based on FLL is presented. The theory analysis and the design of parameters are covered in this section as well. In Section IV, validation of the proposed method is assessed through simulation and experiment results. Finally, the conclusion is presented in Section V.

II. Control Strategy Design and Analysis on PCC Voltage Response after Islanding

A. Control Design for Inverter in Microgrid

Fig. 1 shows the power stage and control algorithm of the inverter used in single-phase microgrid. With different work mode for microgrid, the strategy and objective are different.

1). Control Design for Island Mode

Reliable power supply to local loads with pure sinusoidal voltage is the basic goal for island mode. For single phase inverters, the capacitor voltage and inductance current are used as feedback signals and send to double closed-loop control as shown in Fig. 1. Proportional-resonant (PR) controller is employed due to its performance for tracking fundamental as well as harmonic components caused by non-linear loads [22] (in this paper, only linear parallel RLC load is considered for islanding detection). Voltage and current PR controller are as follows respectively,

$$G_v(s) = k_{Pv} + \sum_{k=1,3,5,7} \frac{k_{Rvk} \cdot s}{s^2 + \omega_c s + (k \cdot \omega_o)^2} \quad (1)$$

$$G_i(s) = k_{Pi} + \sum_{k=1,3,5,7} \frac{k_{Rik} \cdot s}{s^2 + \omega_c s + (k \cdot \omega_o)^2} \quad (2)$$

where k_{Pv}, $k_{Pi}$are the proportional coefficients; k_{Rvk}, k_{Rik} are the fundamental resonant coefficients (k=1) and kth harmonic resonant coefficients; ω_c and ω_o represent the cut-off frequency and resonance angular frequency, respectively.

In island mode, the reference voltage and frequency (or phase) are given as v_{Island} and θ_{Island} in Fig.1 respectively.

2). Control Design for Synchronous Mode

Synchronous mode is defined as the transition between island and grid-connected mode of operation. In this mode, the reference voltage and phase are set to be voltage and phase at PCC from PLL unit [22]. Hence, the synchronization process between the output voltage and grid voltage smooth the transition from island to grid-connected mode.

3). Control Design for Grid Connected Mode

Generally, microgrid is considered as a PQ node in grid-connected mode to control the exchange active/reactive power (*P*/*Q*) with the main utility. In the rotating reference frame, as the v_q equals to zero when it is synchronized with the grid voltage, the active and reactive reference current can be calculated from (3) and (4), respectively [24].

$$i_d = \frac{2P_{ref}}{v_d} \tag{3}$$

$$i_q = \frac{2Q_{ref}}{v_d} \tag{4}$$

where P_{ref}, Q_{ref} indicate power reference exchange between the microgrid and the main utility; v_d, v_q, i_d, i_q represent the d-axis and q-axis components for current and voltage, respectively.

According to different active and reactive power reference, reference current can be generated through dq/αβ transformation based on the phase angle from PLL shown in Fig. 1. What should be noted here is the reference phase of current is modified through the islanding detection method (IDM) model based on the PCC voltage phase angle.

With the reference current, PR controller in (2) is utilized here to regulate the power exchanging between utility grid and microgrid.

B. PCC Voltage and Frequency Response after Islanding

Eq. (5) and (6) represent the active and reactive power consumed for parallel RLC load when microgrid is connected to utility grid with constant power control, respectively [25].

$$P_L = P_{MG} + P_G = \frac{\mathrm{V^2_{PCC}}}{\mathrm{R}} \tag{5}$$

$$Q_L = Q_{MG} + Q_G = \mathrm{V^2_{PCC}}\left[\left(2\pi f_{\mathrm{g}}\mathrm{L}\right)^{-1} - 2\pi f_{\mathrm{g}}\mathrm{C}\right] \tag{6}$$

where P_L, Q_L, P_{MG}, Q_{MG}, P_G, Q_G are the active/reactive power for RLC load, microgrid output power and injected power to utility grid shown in Fig.1 respectively; $\mathrm{V_{PCC}}$ and f_g are the PCC voltage and frequency.

Thus, the frequency and magnitude of PCC voltage is seriously affected both by power state and the characteristics of local load after islanding. But the basic principle is that the voltage magnitude and frequency at PCC will change until the output power matches the local consumption after islanding. From (5), if the output active power doesn't match the requirement, PCC voltage will certainly increase or decrease until P_{MG}=P_L. Similarly, the frequency has to change and stabilize at a frequency where the output reactive power equals to the demand. But different from that the magnitude is just dominated by the active power mismatch, the frequency will flux both for the active and reactive power mismatch, if we combine (5) and (6).

The other factor affecting frequency at PCC is the characteristics of local load. The quality factor for RLC load is defined as below,

$$Q_f = \mathrm{R}\sqrt{\frac{\mathrm{C}}{\mathrm{L}}} = 2\pi f_o \mathrm{RC} = \frac{\mathrm{R}}{2\pi f_o \mathrm{L}} \tag{7}$$

where $f_o = 1/2\pi\sqrt{LC}$is the natural resonant frequency of the parallel RLC. Thus, eq. (6) can be modified as follows,

$$Q_L = \mathrm{V^2_{PCC}}\left[\frac{Q_f}{\mathrm{R}}\left(\frac{f_o}{f_{\mathrm{g}}} - \frac{f_{\mathrm{g}}}{f_o}\right)\right] = P_L Q_f \left(\frac{f_o}{f_{\mathrm{g}}} - \frac{f_{\mathrm{g}}}{f_o}\right) \tag{8}$$

The active and reactive mismatch power after islanding can be expressed as follows,

$$\Delta P = P'_L - P_L = P_{MG} - P_L \tag{9}$$

$$\Delta Q = Q'_L - Q_L = Q_{MG} - Q_L \tag{10}$$

where ΔP, ΔQ, P'_L, Q'_L represent the active/reactive mismatch power and the consumed active/reactive power after islanding, respectively. For constant power control method, $P'_L = P_{MG}$ and $Q'_L = Q_{MG}$ are the objective after islanding.

Assumed that the reactive power matches well while the active power does not, the following equation can be obtained from (8) and (9):

$$\Delta P = \frac{\left(f - f_{\mathrm{g}}\right)\left(f_o^2 + f f_{\mathrm{g}}\right)}{f\left(f_o^2 - f_{\mathrm{g}}^2\right)} P_{MG} \tag{11}$$

where *f* indicates the stable frequency after islanding.

It indicates that the influence on frequency from the active power mismatch is not only determined by the sign of the active mismatch power and the output active power, but also determined by the relationship between the load resonance frequency and utility frequency at PCC.

Similarly, assumed that the active power matches well while the reactive power does not, the following equation can be obtained from (8) and (10):

$$\Delta Q = \frac{\left(f_{\mathrm{g}} - f\right)\left(f_o^2 + f f_{\mathrm{g}}\right)}{f_{\mathrm{g}}\left(f_o^2 - f^2\right)} Q_{MG} \tag{12}$$

Except for the sign of the reactive power mismatch and the output reactive power, there is also a relationship between the resonance frequency and the steady frequency after islanding. From (11) and (12), the voltage and frequency response can be concluded in Table I.

For a parallel RLC load, the transfer function from current to voltage (scilicet the form of RLC in *s* domain) is defined in (13) as follows,

$$\mathrm{H}(s) = \mathrm{Z_L}(s) = \frac{\mathrm{U}(s)}{\mathrm{I}(s)} = \frac{\mathrm{RL}\cdot s}{\mathrm{RLC}\cdot s^2 + \mathrm{L}\cdot s + \mathrm{R}} \tag{13}$$

The corresponding phase-frequency curve for three different Q_f is shown in Fig. 2. In grid-connected mode, the stable frequency equals to the frequency of utility voltage (f_g) for any Q_f and output power factor angle θ_{PF}. The operation points are marked with *a*, *c* and *e* on each curve. While microgrid with constant θ_{PF} (constant power controlled) transfers to island

TABLE I. RELATIONSHIP BETWEEN POWER STATE AND PCC VOLTAGE

Power state	Magnitude		Stable frequency
ΔP=0 ΔQ=0	unchanged		unchanged（f=f_g）
ΔP=0 ΔQ>0	unchanged		Q_{MG}>0: f decrease and f<f_o Q_{MG}<0: f decrease and f>f_o
ΔP=0 ΔQ<0	unchanged		Q_{MG}>0: f increase and f<f_o Q_{MG}<0: f increase and f>f_o
ΔP>0 ΔQ=0	increase		Q_{MG}>0: f increase and f<f_o Q_{MG}<0: f decrease and f>f_o
ΔP<0 ΔQ=0	decrease	P_{MG}>0	Q_{MG}>0: f increase and f<f_o Q_{MG}<0: f decrease and f>f_o
		P_{MG}<0	Q_{MG}>0: f increase and f<f_o Q_{MG}<0: f decrease and f>f_o
ΔP≠0 ΔQ≠0	change		depends on ΔP, ΔQ, P_{MG} and Q_{MG}

Note: Q_{MG}>0/Q_{MG}<0 mean microgrid output inductive/capacitive reactive power respectively; P_{MG}>0 /P_{MG}<0 mean active power exporting to/ absorbing from utility grid.

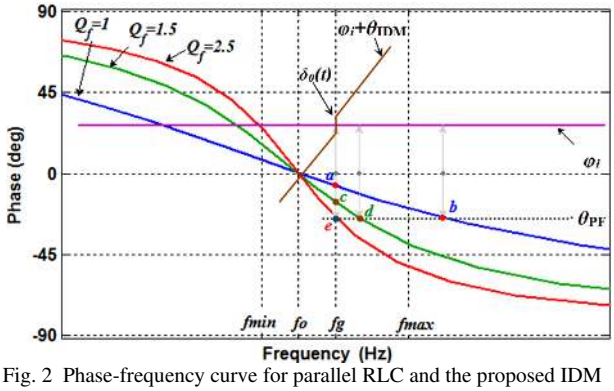

Fig. 2 Phase-frequency curve for parallel RLC and the proposed IDM

mode, the frequency will deviate until the equation below is satisfied,

$$\theta_L(f) = \theta_{\mathrm{PF}} \tag{14}$$

where θ_{PF} and $\theta_L(f)$ are the power factor angle and load impedance angle at stable frequency after islanding. Only for unity power factor, the frequency will stabilize at the natural resonant frequency f_o of the load.

As shown in Fig. 2, the frequency will be drifted up after islanding to the stable operation points where the intersection of the load Phase-frequency curve and output power factor angle marked as b, d and e on curves for three different power qualities respectively. The figure shows, in the case of power mismatch, the stable frequency for Q_f=1 will exceed the upper frequency threshold f_{max} while for Q_f=1.5 will not. In the case of active\reactive power match for Q_f =2.5, the stable frequency doesn't change at all. It can be concluded that the higher power quality for a certain power mismatch, the little frequency deviation will be. On the other hand, the frequency will not change if the power matches well. As a result, high load power quality and power match are the worst case for islanding detection. According to IEEE Standard 929 [25], Q_f <2.5 can represent the power quality of general loads in reality. As a result, parallel RLC load with Q_f=2.5 is used for islanding detection in this paper.

III. IDM BASED ON FLL USING FREQUENCY POSITIVE FEEDBACK

In order to drive the frequency of PCC voltage exceeding the permissible range, frequency based islanding detection method has to change the frequency of output current actively.

A. IDM Based on Frequency Positive Feedback

Without considering the little steady error of control method, the output current can be assumed to reference current defined below,

$$\begin{aligned} \mathrm{I}_{ref} &= I * \sin\left[2\pi f_{\mathrm{g}}\mathrm{t} + (\varphi_i + \theta_{\mathrm{IDM}})\right] \\ &= I * \sin\left[2\pi f_{\mathrm{g}}\mathrm{t} + (\theta_{\mathrm{IDM}} - \theta_{\mathrm{PF}})\right] \end{aligned} \tag{15}$$

where I is the magnitude of reference current; f_g, φ_i, θ_{PF} are the locked frequency of PCC voltage, phase angle of reference current and power factor angle, respectively; θ_{IDM} is the phase shift generated from IDM unit.

The phase shift is generated based on frequency positive feedback as follows,

$$\theta_{\mathrm{IDM}} = m * (f - f_n) \tag{16}$$

where f_n and f are the nominal line frequency and the measured instantaneous frequency at PCC; m is the acceleration coefficient for frequency positive feedback.

From (16), the shift phase will be positive once the PCC frequency is greater than nominal line frequency. Then, the positive phase shift will drift the reference frequency higher if the sum of θ_{IDM} and φ_i is positive as shown in Fig.2. And the greater PCC frequency will lead a larger positive phase shift further until PCC frequency exceeding the upper limitation. Similarly, the reference frequency will be lower and lower once PCC frequency is smaller than nominal line frequency. This is the mechanism of frequency positive feedback.

As it is shown in Fig.2, in order to drift the frequency out of the allowable range, there must be no stable operation point within the range at least or no stable operation point at all. Therefore, the change of reference phase versus frequency deviation must be faster than the change of load impedance angle. Hence, the following relationship should be satisfied,

$$\frac{\mathrm{d}\theta_{\mathrm{IDM}}}{\mathrm{d}f}\Big|_{f=f_{\mathrm{g}}} > \left(\frac{\mathrm{d}\theta_{\mathrm{L}}}{\mathrm{d}f}\Big|_{f=f_{\mathrm{g}}}\right)_{\max} \tag{17}$$

The solution can be derived from (13), (16) and (17),

$$m > \left(\frac{Q_f\left(\frac{f_o}{f_{\mathrm{g}}^2} + \frac{1}{f_o}\right)}{1 + Q_f^2\left(\frac{f_o}{f_{\mathrm{g}}} - \frac{f_{\mathrm{g}}}{f_o}\right)} * \frac{180}{\pi}\right)_{\max} \tag{18}$$

It can be obtained from the curve in Fig.2 that the value will be maximum when the resonance frequency equals to the utility frequency (f_o=f_g).

But if the power matches exactly, PCC frequency equals to nominal line frequency. In this case, the phase shift equals to zero and can be only stimulated by the measurement and sample errors in practice [5, 16]. The islanding detection may be lengthen or even fail. In [16], an additional initial phase shift in Eq. (19) is used to solve this issue.

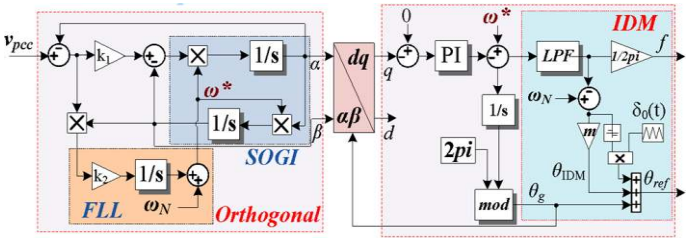

Fig. 3 Detail control diagram for proposed IDM

$$\theta_{\mathrm{IDM}} = m * (f - f_n) + \mathrm{sign}(f - f_n)\delta_0\,(\mathrm{t}) \qquad (19)$$

where δ_0 (t) is the initial phase perturbation and sign(f-f_n) is the sign of error between measured and nominal frequency.

However, constant initial phase shift could be counterweighed by the power factor angle for constant power control strategy in microgrid [21]. So the initial phase shift applied in this paper is defined as a low frequency triangular signal below,

$$\delta_0\,(\mathrm{t}) = \begin{cases} \dfrac{2\delta_0}{\mathrm{T}} * \mathrm{t}, & \dfrac{\mathrm{N}}{2}\mathrm{T} \le t < \dfrac{(\mathrm{N}+1)}{2}\mathrm{T} \\ \delta_0 - \dfrac{2\delta_0}{\mathrm{T}} * \mathrm{t}, & \dfrac{(\mathrm{N}+1)}{2}\mathrm{T} \le t < \dfrac{(\mathrm{N}+2)}{2}\mathrm{T} \end{cases} \qquad (20)$$

$$(\mathrm{N} = 0,2,4,\cdots)$$

where T is the period of triangular signal; δ_0 is a small constant perturbation.

With the proposed method, the control unit with slash shade in Fig. 1 can be expressed in detail as Fig. 3.

B. IDM Effect Analysis Using PLL and FLL

From (15), another element affecting current reference phase angle is the frequency locked from PCC voltage. Usually, PLL based on second order general integrator (SOGI) is used in single phase system to generate the phase angle for reference current [27]. But just as the frequency based IDM discussed above, PCC frequency is variable with the output current frequency variation after islanding, especially active IDM is used. With the SOGI module shown in Fig. 3, the transfer function is defined as,

$$\mathrm{H}_\alpha(s) = \frac{\mathrm{v}_\alpha(s)}{\mathrm{v}_{\mathrm{pcc}}(s)} = \frac{\mathrm{k}_1\omega s}{\mathrm{s}^2 + \mathrm{k}_1\omega s + \omega^2} \qquad (21)$$

where ω is the resonance frequency of SOGI.

Generally, the resonance frequency is fixed to nominal line frequency. The corresponding frequency response curve is shown in Fig.4.

It can be obtained that the SOGI unit will lead to phase error if the input frequency doesn't equal to the resonance frequency. In detail, the phase error is positive if the input frequency is lower than resonance frequency while the error is negative if the frequency is higher than resonance frequency. As a result, during the active detection process after islanding, the SOGI unit will certainly be inaccurate because of the variation of PCC frequency. Fig. 5 shows the reference phase and the corresponding reference current considering the generated phase shift and the phase error caused by PLL.

According to the IDM based on frequency positive feedback proposed above, the phase shift θ_{IDM} is negative if PCC frequency is lower than nominal line frequency at t=t1

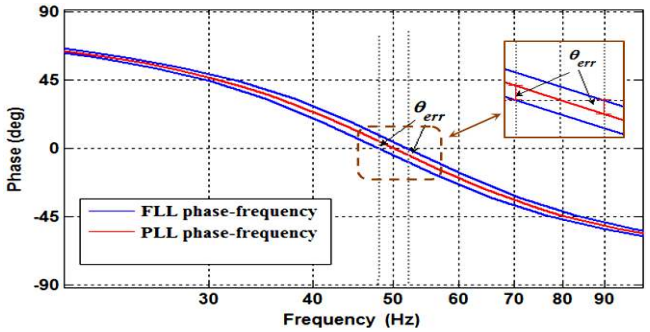

Fig. 4 phase-frequency curve for PLL (red) and FLL (blue)

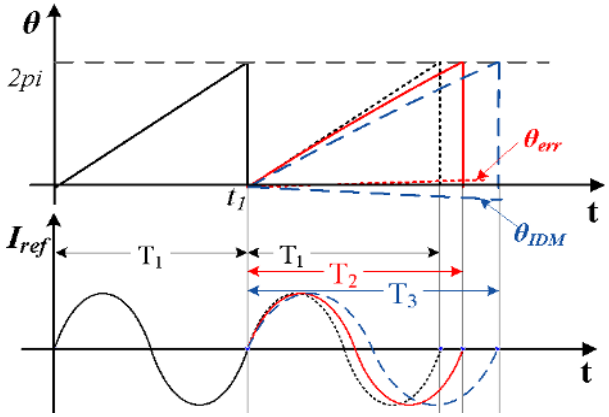

Fig.5 The effect of the phase error

labeled in Fig.5. However, the phase error θ_{err} caused by the SOGI unit is positive at the same period. Thus, this phase error will counteract the phase shift and weaken the positive effect of the frequency feedback. Thereby, the real period is T_2 if both the phase shift and phase error are considered rather than the period T_3 when only phase shift is considered. Therefore, the change of frequency will be slower and the detection time will be longer. The same conclusion can be obtained in the case that PCC frequency is higher than nominal line frequency.

In order to solve this problem, Frequency-Locked Loop (FLL) is introduced to SOGI unit to modify the constant resonance frequency in this paper as Fig.3 [28]. Here, the dynamic frequency deviation from FLL is added to nominal angular frequency to improve the stability. The corresponding phase-frequency curve is also shown in Fig. 4. As the resonance frequency is dynamic changed, there is no phase error no matter the input frequency changes or not.

Except for the phase error, another element affecting the active IDM is PCC frequency f_g according to (15). Based on FLL presented in Fig.3, the reference frequency is also modified. This process contributes to the frequency lock speed in contrast with conventional PLL. The ramp response for conventional PLL and modified unit with FLL are both drawn in Fig.6. It shows that the ramp response for FLL unit is more rapid than that of conventional PLL. This rapid response can improve the effect of frequency positive feedback.

C. NDZ Analysis of the Proposed Method

Load parameter space based on the load quality factor and resonant frequency (Q_f versus f_0) is utilized to evaluate the NDZ for the proposed IDM. According to Fig.2, the following phase criteria should be met,

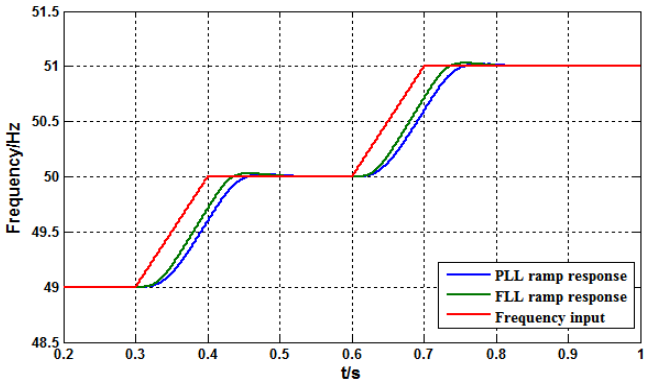

Fig.6 Ramp response curve for PLL and FLL

$$\theta_{\mathrm{L}}(f) = \theta_{\mathrm{PF}} + \theta_{\mathrm{IDM}} \tag{22}$$

The following equation can be obtained from (13), (16), (22),

$$f_o^2 + \frac{[\tan(\theta_{\mathrm{IDM}}) + \tan(\theta_{\mathrm{PF}})]f}{[1 - \tan(\theta_{\mathrm{IDM}})\tan(\theta_{\mathrm{PF}})]Q_f} f_o - f^2 = 0 \tag{23}$$

where $\tan(\theta_{PF})$ is the constant value determined by power factor. Adjusting the frequency after islanding to the threshold (f_{max} and f_{min}) [28], the relationship for load quality factor and resonance frequency with different power factor and positive acceleration coefficient calculated from (18) is shown in Fig.7. The area between two curves with the same power factor and acceleration parameter (the same color) is the NDZ corresponding to the given parameters. In Fig.7 (a), the boundary marked with star separates the NDZ and non-NDZ area with the same positive acceleration coefficient (m=7) and random power factor. From the details of the NDZ curve in Fig.7 (b), it can be obtained that there will be no NDZ for load with quality factor less than 2.62 using the proposed IDM.

Another conclusion from the NDZ curves with m=7 and m=15 is that the larger the positive acceleration coefficient, the narrower the corresponding NDZ. But the perturbation and distortion of the output current during grid-connected mode will be increased meanwhile.

D. Analysis for multiple inverters and three phase system

In the case of multiple inverters using the proposed method, each inverter will introduce the initial disturbance and positive feedback. No matter the sign of initial phase shift at the same time is the same or not, the sum will not counteract each other because the nonlinear of sinusoidal. Hence, the initial phase disturbance to PCC frequency is still effective. After islanding, PCC voltage equals to the sum of each output current multiplied by load impedance. For each inverter, the angle deviation of output current is determined by PCC frequency and its own P\Q reference shown in Eq. (15). So the deviation angle will drift the frequency in the same direction as the same PCC frequency. Although different IDM and FLL parameters lead to different frequency deviation speed for each inverter, the sum of the current with the same frequency deviation in direction still leads the same deviation to PCC frequency in direction. Moreover, small voltage fluctuation owing to the slight frequency differ of each output current contributes to the instability. Therefore, the proposed method is still effective for multiple inverters.

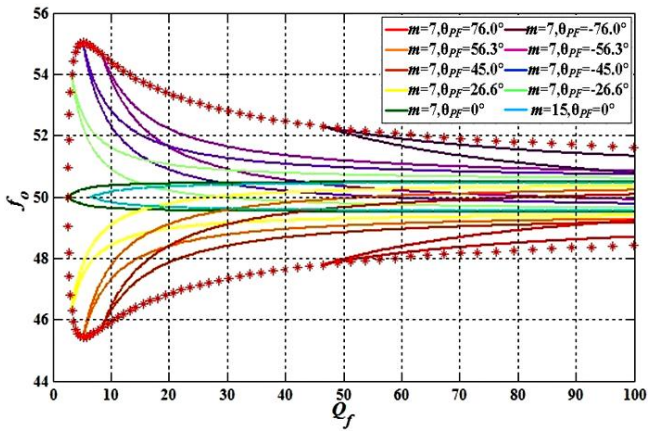

(a) NDZ with different power factor and acceleration coefficient

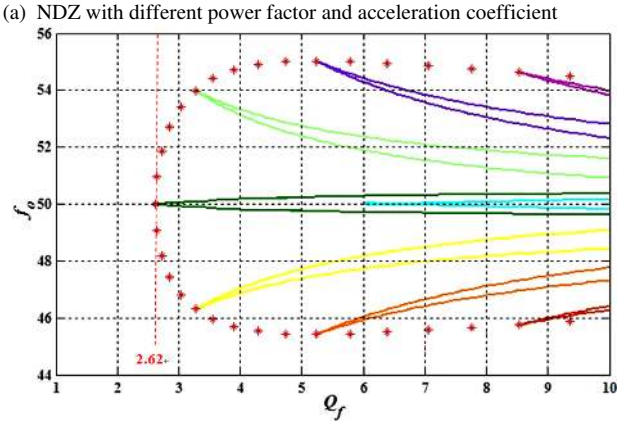

(b) Zoom in of the NDZ

Fig.7 NDZs of the proposed IDM with different parameters

Although this method is analyzed and used for single phase inverter, it is also effective for three phase inverter using similar control strategy based on PLL in grid-connected mode.

IV. Experiment Results and Analysis

The proposed IDM, as the structure and control algorithms, were implemented in MATLAB/Simulink based on Fig.1. The proposed strategy is validated in a dSPACE 1006 based real-time platform. The setup used consists of a constant power controlled single-phase inverter and a parallel RLC load. The power stage parameters and corresponding control parameters are listed in Table II.

Three scenarios with different islanding detection methods are simulated and assessed by considering the case with active/reactive power match as the worst case for islanding detection.

Scenario (S_1): Passive islanding detection method.

Scenario (S_2): PLL-based islanding detection method using frequency positive feedback.

Scenario (S_3): FLL-based islanding detection method using frequency positive feedback.

For the parallel RLC load (Q_f = 2.5) given in Table II, the reference active/reactive power is 920W/-500Var. For all the three planned scenarios, the output active/reactive power is controlled to be the reference value in grid-connected mode in order to match the parallel RLC load. At t=0.2s, the main utility is abnormal and island occurs. O/UF with the frequency limitation 50±0.5Hz was used as the islanding detector.

Fig. 8 shows the results, including PCC voltage, output active/reactive power, PCC frequency, the islanding and trip

TABLE II. POWER STAGE AND CONTROL PARAMETERS

DC	*LC Filter*	*Utility grid*	*Load*	
Vdc(V)	L(mH)/C(μF)	Vrms(V)/*f*(Hz)	R(Ω)/L(mH)/C(μF)	
650	3.6/13.5	230/50	57.5 /81.6/154.3	
		Voltage Controller		
k_{pV}	k_{rV1}	k_{rV3}	k_{rV5}	k_{pI}
0.005	80	45	30	50
		IDM Parameters		
m	δ_0	T (s)	f_{max}(Hz)	f_{min}(Hz)
7	1.5°	1	50.5	49.5
		Current Controller		
k_{rI1}	k_{rI3}	k_{rI5}	ω_c (rad/s)	
160	35	25	8	
		FLL Parameters		
k1	*k2*	$k_{p\text{-}PLL}$	$k_{i\text{-}PLL}$	ω_N (rad/s)
1	-0.4	0.7	0.2	100pi
AFD	SMS *Parameters*		*Line Impedance*	
cf_0	θm	f_m(Hz)	r(Ω)/*l* (mH)	
0.03	10°	53	0.1/1	

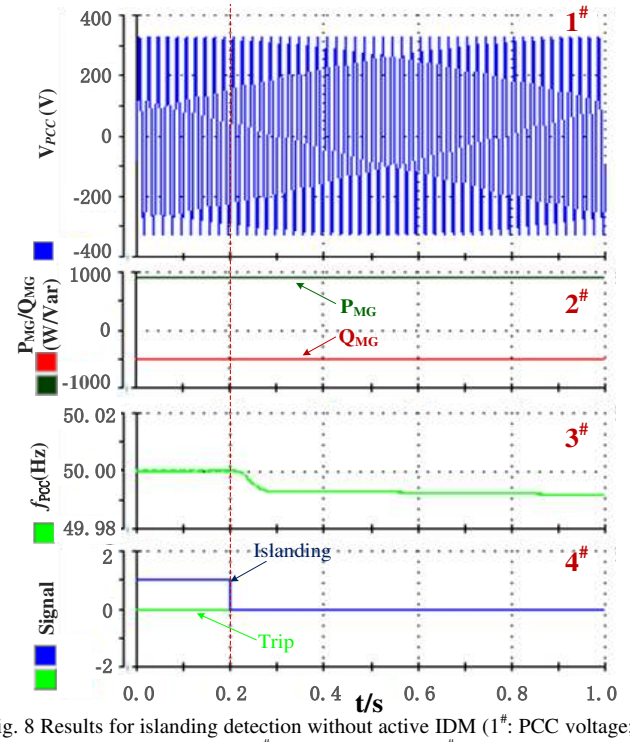

Fig. 8 Results for islanding detection without active IDM (1#: PCC voltage; 2#: output active/reactive power; 3#: PCC frequency; 4#: Islanding and trigger signal)

signal, corresponding to scenario S_1 with a passive islanding detection method. It shows that the inverter is constant power controlled and the output power follows the reference value properly. But the voltage at PCC is stable after islanding as the output power matches the local load. The PCC frequency just slightly changes (within 0.02Hz) after islanding. As a result, it is not enough to trigger O/UF detector and indicate the islanding. It can be seen that it will be located in NDZ for this scenario S_1.

Fig.9 shows the similar results after islanding for scenario S_2 with PLL-based IDM using a frequency positive feedback method. As the frequency is a positive feedback, the frequency at PCC is drifted away from nominal value and reaches the threshold rapidly. From the details of frequency and signal waveforms, islanding can be detected at t=0.272s. As the frequency changes, PCC voltage marked with 1# has also

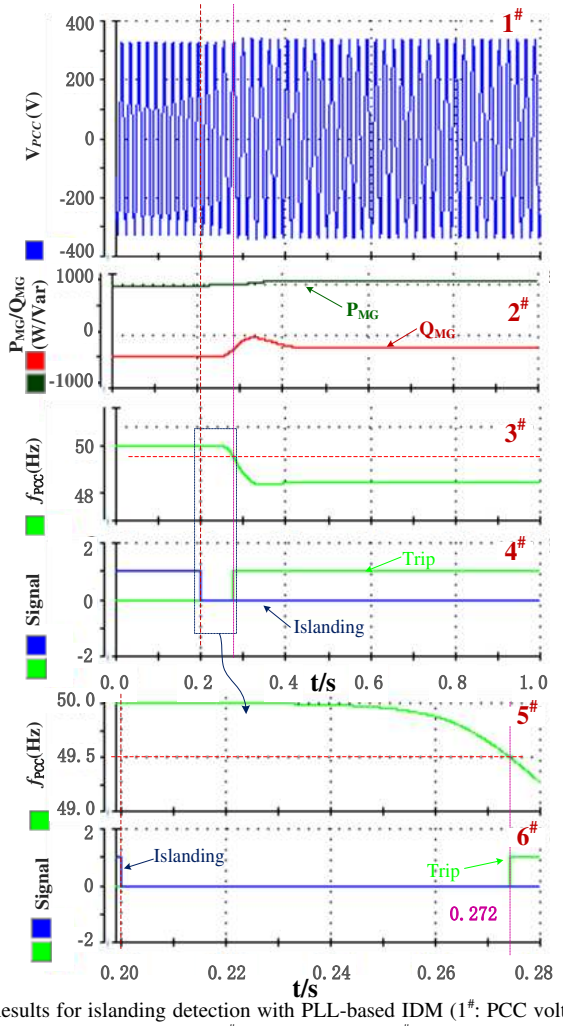

Fig. 9 Results for islanding detection with PLL-based IDM (1#: PCC voltage; 2#: output active/reactive power; 3#: PCC frequency; 4#: Islanding and trigger signal; 5#: PCC frequency zoom in; 6#: Trigger signal zoom in)

changed a little due to the magnitude response for RLC is frequency dependence. Meanwhile, the output active/reactive power also changes along with the frequency deviation.

Fig.10 shows the third scenario S_3 with FLL-based IDM using frequency positive feedback proposed in this paper. As it can be seen from the results, PCC frequency also changes similarly to the PLL-based method, but the rate of change of frequency is faster. At t=0.248s, islanding can be detected. The output power and the PCC voltage change a lot both than the passive method and PLL-based method as the frequency changes more severely. From Fig. 10, the frequency increased after islanding while it decreased in Fig. 9. It is determined by the initial frequency error at the beginning whether the frequency increases or decreases.

For parallel RLC load with different quality factor, the detection trigger signal using the proposed detection method is illustrated in Fig. 11. Corresponding to Qf=1.5, Qf=2.5, Qf=3, the detection time are t=0.241s, t=0.251s, t=0.257s respectively. It shows that the larger the quality factor Q_f, the longer will it cost for islanding detection.

Additionally, nonislanding event was considered to test the accuracy of the proposed method. Fig. 12(a), (b) shows the PCC frequency when switching on (t_1)\cutting off (t_2) resistive load R=10Ω and capacitive load C=470μF, respectively. It can

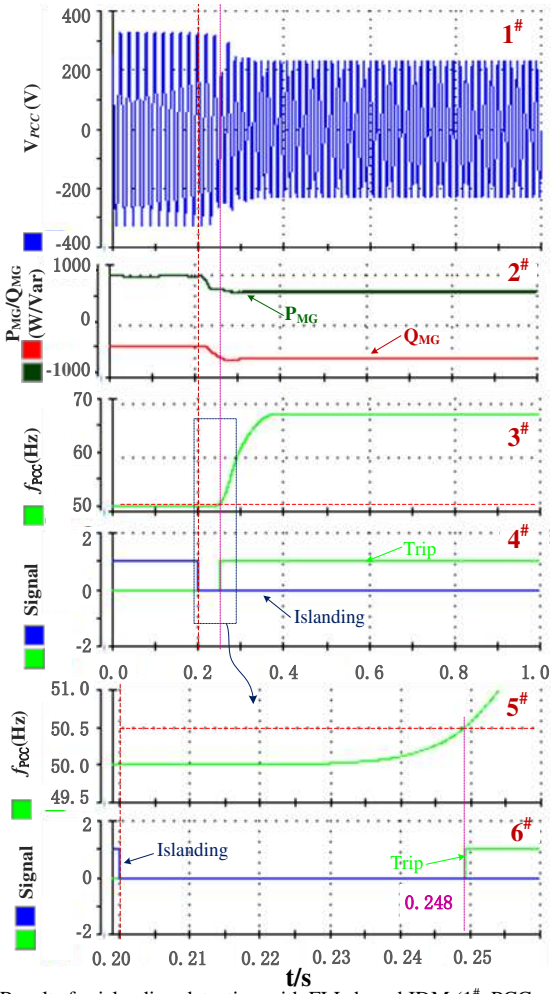

Fig. 10 Results for islanding detection with FLL-based IDM (1#: PCC voltage; 2#: output active/reactive power; 3#: PCC frequency; 4#: Islanding and trigger signal; 5#: PCC frequency zoom in; 6#: Trigger signal zoom in)

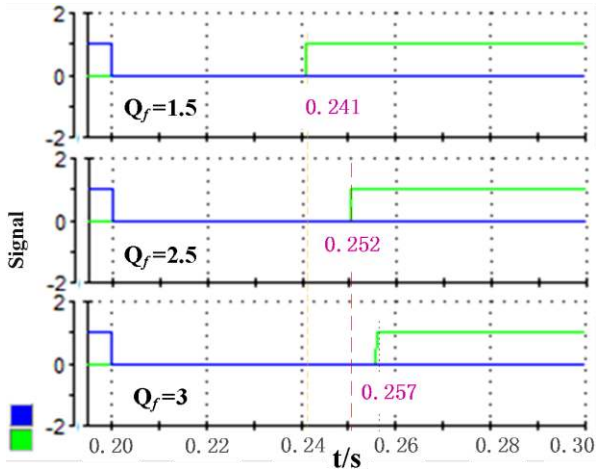

Fig. 11 Trigger signal for different Q_f using proposed method

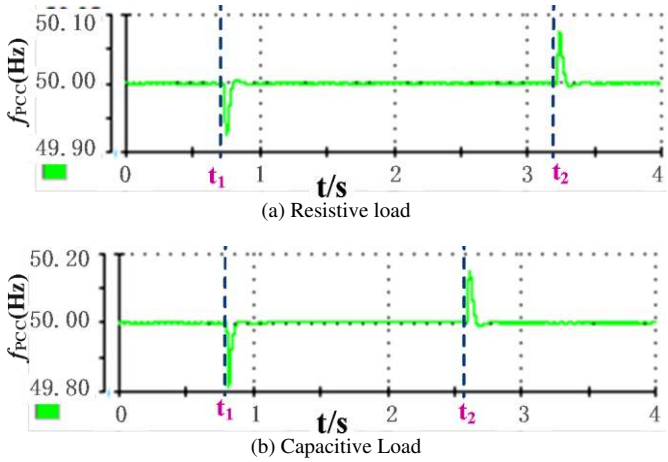

(a) Resistive load

(b) Capacitive Load

Fig. 12 Frequency deviation for sudden load changing

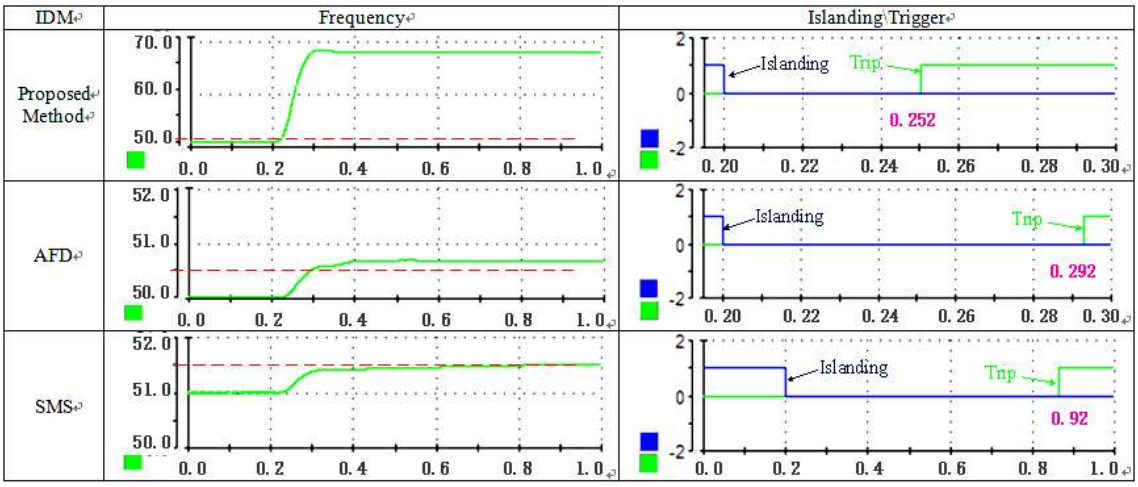

Fig. 13 Comparison results with AFD and SMS islanding detection method

be seen PCC frequency will change because of the sudden load. But it doesn't exceed the allowance limitation. One reason is that orthogonal and LPF unit used in Frequency locked unit filter the change of frequency. However, for large load in weak grid, false detection is possible as mentioned in [14]. Some confirm process such as time-delay has to be applied to increase the accuracy at the expense of detection time.

Fig. 13 shows the results comparing with AFD and SMS method including the change of PCC frequency and trigger signal. The parameters used for AFD and SMS are listed in Table II. It can be seen that the proposed method based on FLL could detect islanding at t=0.252s while the detection time is t=0.292s for AFD. But for SMS method, it costs a much longer time to detect islanding at t=0.92. Therefore, AFD is more effective than SMS for constant power

controlled inverter because the power regulation could counteract the angle from SMS. From the results, the positive feedback method based on FLL is effective and fast.

V. Conclusion

This paper proposed an active islanding detection method for single phase inverters used in microgrids. This method , according to the analysis of PCC voltage and frequency response after islanding, utilizes frequency positive feedback and FLL which makes the detection accurate and fast considering that the frequency is time variable during the detection process. Additionally, by a low frequency variable initial disturbance angle instead of constant one, this method solves the issue that it could be counterweighed by the power regulation for constant power controlled inverter when microgrid connected to utility grid. Three scenarios were used to verify the effectiveness. The results have shown the performance of the proposed islanding detection method for constant power controlled inverters used in microgrids.

VI. REFERENCES

[1] J. M. Guerrero, M. Chandorkar, T. Lee, and P. C. Loh, "Advanced control architectures for intelligent microgrids--Part I: Decentralized and hierarchical control," *IEEE Trans. Ind. Electron*., vol.60, no. 4, pp. 1254-1262, Apr. 2013.

[2] Canbing Li, Chi Cao, Yijia Cao, Yonghong Kuang, Long Zeng, Baling Fang, "A review of islanding detection methods for microgrid," *Renewable and Sustainable Energy Reviews*, vol. 35, pp.211-220, 2014

[3] C. L. Chen, Y. Wang, J. S. Lai, Y. S. Lee, and D. Martin, "Design of parallel inverters for smooth mode transfer microgrid applications," *IEEE Trans. Power Electron.*, vol. 25, no. 1, pp. 6-15, Jan. 2010.

[4] W. Xu, G. Zhang, Li, W. Wang, G. Wang, and J. Kliber, "A power line signaling based technique for anti-islanding protection of distributed generators—Part I: Scheme and analysis," *IEEE Trans. Power Del.*, vol. 22, no. 3, pp. 1758-1766, Jul. 2007.

[5] M. Ropp and W. Bower, "Evaluation of islanding detection methods for photovoltaic utility interactive power systems," *Int. Energy Agency Implementing Agreement Photovoltaic Power Syst. Paris, France*, Tech. Rep. IEA PVPS T5-09, 2002.

[6] F. D. Mango, M. Liserre, A. D. Aquila, and A. Pigazo, "Overview of anti islanding algorithms for PV systems. Part I: Passive methods," in *Proc. 12th Int. Conf. Power Electron. Motion Control EPE-PEMC*, Slovenia, pp. 1878–1883, 2006.

[7] H. H. Zeineldin, J. L. Kirtley, "Performance of the OVP/UVP and OFP/UFP Method with Voltage and Frequency Dependent Loads," *IEEE Trans. Power Del.*, vol. 24, no. 2, pp. 772-778, Apr. 2009.

[8] Singam B., Hui L.Y., "Assessing SMS and PJD Schemes of Anti Islanding with Varying Quality Factor," in *Proc. IEEE Power and Energy Conf.*, pp. 196-201, Nov. 2006.F. De mango, M. Liserre, and A. D. Aquila, "Overview of Anti Islanding Algorithms for PV Systems. Part II: Active Methods," in *Proc. IEEE Power Electronics and Motion Control Conf.*, pp. 1884–1889, Jan. 2007.

[9] Redfern M.A., Usta O., Fielding G., "Protection against loss of utility grid supply for a dispersed storage and generation unit," *IEEE Trans. Power Del.*, vol. 8, no. 3, pp. 948-954, Jul. 1993.

[10] F. D. Mango, M. Liserre, A. D. Aquila, "Overview of Anti-Islanding Algorithms for PV Systems. Part II: Active Methods," in *Proc. 12th Int. Conf. Power Electron. Motion Control EPE-PEMC*, Slovenia, pp. 1884-1889, 2006.

[11] Ropp M.E., Begovic M., Rohatgi A., "Analysis and performance assessment of the active frequency drift method of islanding prevention," *IEEE Trans. Energy Conversion*, vol. 14, no. 3, pp. 810-816, Sep. 1999.

[12] Yu Byunggyu, Matsui Mikihiko, Yu Gwonjong, "A combined active anti-islanding method for photovoltaic systems," *Renewable Energy*, vol.33, no.5, pp. 979-985, May 2008.

[13] H. H. Zeineldin and S. Kennedy, "Sandia Frequency-Shift Parameter Selection to Eliminate Non detection Zones," *IEEE Trans. Power Del.*, vol. 24, no. 1, pp. 486-488, Jan. 2009.

[14] Xiaoyu Wang, Walmir Freitas,"Impact of Positive-Feedback Anti-Islanding Methods on Small-Signal Stability of Inverter-Based Distributed Generation," *IEEE Trans. energy conversion*, vol. 23, no. 3, pp. 923-931, Sep. 2008

[15] F. Liu, Y. Kang, Y. Zhang, S. Duan, X. Lin, "Improved SMS islanding detection method for grid-connected converters," *IET Renew. Power Gener.* vol. 4, no. 1, pp. 36-42, 2010

[16] G. Hung, C. Chang, and C. Chen, "Automatic phase-shift method for islanding detection of grid-connected photovoltaic inverter", *IEEE Trans. Energy Conversion*, vol. 18, no.1, pp. 169-173, Mar. 2003.

[17] Bifaretti S., Lidozzi A., Solero L., Crescimbini F. "Anti-Islanding Detector based on a Robust PLL," *IEEE Trans. Ind. Application*, vol. 51, no. 1, pp. 398-405, 2015

[18] Velasco D., Trujillo C., Garcera G., Figueres E., "An Active Anti-Islanding Method Based on Phase-PLL Perturbation," *IEEE Trans. Power Electron.,* vol. 26, no. 4,pp.1056-1066, 2011

[19] Andrew J. Roscoe, Graeme M. Burt, Chris G. Bright, "Avoiding the Non-Detection Zone of Passive Loss-of-Mains (Islanding) Relays for Synchronous Generation by Using Low Bandwidth Control Loops and Controlled Reactive Power Mismatches," *IEEE Trans. Smart Grid.,* vol. 5,pp.602-611, 2014

[20] Akhlaghi Shahrokh, Ghadimi Ali Asghar, Akhlaghi, Arash. "A novel hybrid islanding detection method combination of SMS and Q-f for islanding detection of inverter- based DG," *Power and Energy Conference at Illinois (PECI)*, pp. 1-8, 2014

[21] Vasquez, J.C., Guerrero, J.M., Savaghebi, M., Eloy-Garcia, J., Teodorescu, R., "Modeling, Analysis, and Design of Stationary-Reference-Frame Droop-Controlled Parallel Three-Phase Voltage Source Inverters," *IEEE Trans. Ind. Electron.,* vol.60, no.4, pp.1271-1280, Apr. 2013

[22] Sripipat W., Sakorn Po-Ngam, "Simplified Active Power and Reactive Power Control with MPPT for Single-Phase Grid-connected Photovoltaic Inverters," *Electrical Engineering/Electronics, Computer, Telecommunications and Information Technology (ECTI-CON), 11th International Conference on*, pp. 1-4, May, 2014

[23] Yang, M.J., Zhuo, F., Wang, X.W., Guo, H.P., Zhou, Y.J."Research of seamless transfer control strategy of microgrid system," in *Proc. Power Electron. and ECCE Asia (ICPE & ECCE), IEEE 8th Int. Conf. on*, pp. 2059-2066, May, 2011

[24] Xiaolong Chen, Yongli Li, "An Islanding Detection Algorithm for Inverter-Based Distributed Generation Based on Reactive Power Control," *IEEE Trans. Power Electron.*, vol. 29, no. 9, pp. 4672-4683, 2014

[25] *IEEE Recommended Practice for Utility Interface of Photovoltaic (PV) Systems*, IEEE Std. 929-2000, 2000

[26] Ciobotaru M., Teodorescu R., Blaabjerg F., "A New Single-Phase PLL Structure Based on Second Order Generalized Integrator," *Power Electronics Specialists Conference, PESC '06. 37th IEEE*, pp. 1-6, Jun. 2006.

[27] Rodríguez P., Luna A., Candela I., Mujal R., Teodorescu R., Blaabjerg F., "Multiresonant Frequency-Locked Loop for Grid Synchronization of Power Converters Under Distorted Grid Conditions, " *IEEE Trans. Ind. Electron.*, vol. 58, no. 1, pp. 127-138, 2011

[28] Luiz A. C. Lopes, Huili Sun, "Performance Assessment of Active Frequency Drifting Islanding Detection Methods," *IEEE Trans. energy conversion*, vol. 21, no. 1, pp. 171-180, Mar. 2006

Qinfei Sun (Student M' 2015) received his B.S. degree in Electrical Engineering and Automation and M.S. degree in Power System and Automation from College of Information and Electrical Engineering, China Agricultural University, Beijing, China, in 2010, 2012, respectively.

He is currently pursuing the Ph.D. degree with College of Information and Electrical Engineering, China Agricultural University, Beijing, China. He was a guest Ph.D. student with Microgrids Research Program in the Department of Energy Technology, Aalborg University, Aalborg, Denmark, from 2014 to 2015. His current research interests include power electronics for Distributed Generation, operation, control and power quality of microgrid, especially microgrid for rural areas.

Josep M. Guerrero (S'01-M'04-SM'08-FM'15) received the B.S. degree in telecommunications engineering, the M.S. degree in electronics engineering, and the Ph.D. degree in power electronics from the Technical University of Catalonia, Barcelona, in 1997, 2000 and 2003, respectively. Since 2011, he has been a Full Professor with the Department of Energy Technology, Aalborg University, Denmark, where he is responsible for the Microgrid Research Program. From 2012 he is a guest Professor at the Chinese Academy of Science and the Nanjing University of Aeronautics and Astronautics; from 2014 he is chair Professor in Shandong University; and from 2015 he is a distinguished guest Professor in Hunan University.

His research interests is oriented to different microgrid aspects, including power electronics, distributed energy-storage systems, hierarchical and cooperative control, energy management systems, and optimization of microgrids and islanded minigrids. Prof. Guerrero is an Associate Editor for the IEEE TRANSACTIONS ON POWER ELECTRONICS, the IEEE TRANSACTIONS ON INDUSTRIAL ELECTRONICS, and the IEEE Industrial Electronics Magazine, and an Editor for the IEEE TRANSACTIONS on SMART GRID and IEEE TRANSACTIONS on ENERGY CONVERSION. He has been Guest Editor of the IEEE TRANSACTIONS ON POWER ELECTRONICS Special Issues: Power Electronics for Wind Energy Conversion and Power Electronics for Microgrids; the IEEE TRANSACTIONS ON INDUSTRIAL ELECTRONICS Special Sections: Uninterruptible Power Supplies systems, Renewable Energy Systems, Distributed Generation and Microgrids, and Industrial Applications and Implementation Issues of the Kalman Filter; and the IEEE TRANSACTIONS on SMART GRID Special Issue on Smart DC Distribution Systems. He was the chair of the Renewable Energy Systems Technical Committee of the IEEE Industrial Electronics Society. In 2014 he was awarded by Thomson Reuters as Highly Cited Researcher, and in 2015 he was elevated as IEEE Fellow for his contributions on "distributed power systems and microgrids."

Tianjun Jing (M'12) received his B.Sc. in Electrical Engineering from North China Power University, Beijing, China, in 2003 and his Ph.D. in Electrical Engineering from China Agricultural University, Beijing, China, in 2011. He visited the Institute of Energy, Cardiff University, Cardiff, U.K., for one year in 2010. He is the corresponding author of this paper.

His interests are microgrid, renewable generation control, and distribution network automation. He has been working as a lecturer in the College of Information and Electrical Engineering, China Agricultural University since 2011.

Juan C. Vasquez (M'12-SM'15) received the B.S. degree in Electronics Engineering from Autonomous University of Manizales, Colombia in 2004 where he has been teaching courses on digital circuits, servo systems and flexible manufacturing systems. In 2009, He received his Ph.D degree on Automatic Control, Robotics and Computer Vision from the Technical University of Catalonia, BarcelonaTECH, Spain at the Department of Automatic Control Systems and Computer Engineering, where he worked as Post-doc Assistant and also teaching courses based on renewable energy systems, and power management on ac/dc minigrids and Microgrids. Since 2011, he has been an Assistant Professor in Microgrids at the Department of Energy Technology, Aalborg University, Denmark, and he is co-responsible of the Microgrids research programme co-advising more than 10 PhD students and a number of international visitors in research experience. Dr Juan Vasquez is member of the Technical Committee on Renewable Energy Systems TC-RES of the IEEE Industrial Electronics Society and the IEC System Evaluation Group SEG 4 work on LVDC Distribution and Safety for use in Developed and Developing Economies. He is a visiting scholar at the Center for Power Electronics Systems – CPES at Virginia Tech, Blacksburg, VA, USA. He has published more than 100 journal and conference papers and holds a pending patent. His current research interests include operation, energy management, hierarchical and cooperative control, energy management systems and optimization applied to Distributed Generation in AC/DC Microgrids.

Rengang Yang received the B.S. degree from Wuhan University, Wuhan, China, in 1982, the M.S. degree from National Electric Research Institute, Beijing, China, in 1987, and the Ph.D. degree from Tsinghua University, Beijing, in 1993. He is a Professor with the College of Information and Electrical Engineering, China Agriculture University, Beijing.

His main interest and research field are power quality monitoring, harmonic analysis, reactive power compensation and distribution network automation.